



# Degradation of tris(2-chloroethyl) phosphate by ultraviolet-persulfate: Kinetics, pathway and intermediate impact on proteome of *Escherichia coli*



Hua-se Ou<sup>a</sup>, Juan Liu<sup>a</sup>, Jin-shao Ye<sup>a,b,\*</sup>, Lin-lin Wang<sup>a,b</sup>, Nai-yun Gao<sup>c</sup>, Jing Ke<sup>b</sup>

<sup>a</sup>School of Environment, Guangzhou Key Laboratory of Environmental Exposure and Health, and Guangdong Key Laboratory of Environmental Pollution and Health, Jinan University, Guangzhou 510632, China

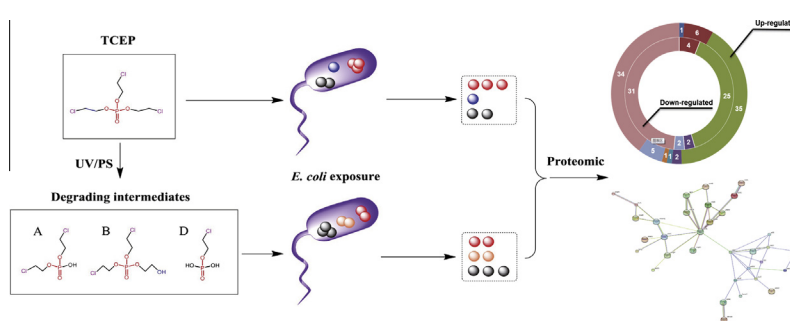
<sup>b</sup>Joint Genome Institute, Lawrence Berkeley National Laboratory, Walnut Creek 94598, CA, USA

<sup>c</sup>State Key Laboratory of Pollution Control and Resources Reuse, College of Environmental Science and Engineering, Tongji University, Shanghai 200092, China

## HIGHLIGHTS

- 254 nm ultraviolet/persulfate induces rapid degradation of TCEP.
- Three intermediates are generated by selective electron-transfer of  $\cdot\text{SO}_4^-$ .
- The impact of TCEP and intermediates on *E. coli* protein expression is compared.
- Degrading TCEP induces less stress on *E. coli* than intact CIP.
- The  $\cdot\text{SO}_4^-$ -based incomplete degradation reduces the toxicity of TCEP.

## GRAPHICAL ABSTRACT



## ARTICLE INFO

### Article history:

Received 7 July 2016

Received in revised form 10 September 2016

Accepted 14 September 2016

Available online 17 September 2016

### Keywords:

Organophosphorus flame retardants  
Ultraviolet  
Persulfate  
Advanced oxidation process  
Proteomics

## ABSTRACT

Organophosphorus flame retardants (OPFRs) are commonly applied in many consumer products, resulting in their widespread distribution in water, soil and indoor air. It is in urgent need of developing efficient and safe removal methods for OPFRs. The degradation kinetics and mechanism of tris(2-chloroethyl) phosphate (TCEP), a representative OPFR, by ultraviolet-persulfate (UV/PS) were explored, and the toxicological assessment of degrading intermediate mixture was performed using isobaric tags for relative and absolute quantitation proteomic technology. The results indicated that UV/PS had a high transformation efficiency of TCEP ( $[\text{TCEP}]_0 = 3.5 \mu\text{M}$ ,  $[\text{S}_2\text{O}_8^{2-}]_0 = 175 \mu\text{M}$ , apparent rate constant reached  $0.1272 \text{ min}^{-1}$ ) with the generations of three primary intermediates, including  $\text{C}_4\text{H}_9\text{Cl}_2\text{O}_4\text{P}$  ( $m/z$  222.97, 224.97),  $\text{C}_6\text{H}_{13}\text{Cl}_2\text{O}_5\text{P}$  ( $m/z$  266.99, 268.99) and  $\text{C}_2\text{H}_6\text{ClO}_4\text{P}$  ( $m/z$  160.98, 162.97), through the selective electron-transfer reactions induced by activated sulfate radical. Compared to that of TCEP, the *Escherichia coli* ATCC11303 exposed to intermediate mixture expressed 64 up-regulated proteins those primarily associated with nutrient import, energy generation, DNA protection and signal transduction. The 86 down-regulated proteins were related to DNA repair, protein turnover and stress response, suggesting that the toxicity of the degrading intermediate mixture decreased significantly. The current study provided insights into the molecular mechanisms of TCEP and its degrading intermediate mixture on *E. coli*, clarifying that the UV/PS degradation is an alternative efficient and safe treatment method for TCEP.

© 2016 Elsevier B.V. All rights reserved.

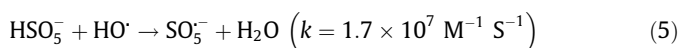
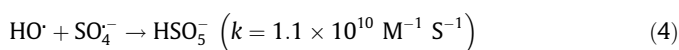
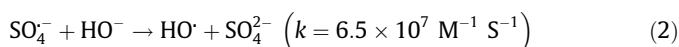
\* Corresponding author at: School of Environment, Guangzhou Key Laboratory of Environmental Exposure and Health, and Guangdong Key Laboratory of Environmental Pollution and Health, Jinan University, Guangzhou 510632, China.

E-mail addresses: [jinshaoye@lbl.gov](mailto:jinshaoye@lbl.gov), [folaye@126.com](mailto:folaye@126.com) (J.-s. Ye).

## 1. Introduction

Flame retardants (FRs) are chemicals applied to regulate the flammability of a variety of consumer products, including vehicles, electronic casings, upholstered furniture, building materials and even baby products [1]. The common FRs included halogenated and organophosphorus flame retardants (OPFRs). In recent years, with the ban of using polychlorinated biphenyls and polybrominated diphenyl ethers FRs in EU and USA, the demands and production yields of OPFRs have increased rapidly [1]. A typical OPFR molecule has a phosphorus backbone with several peripheral moieties, such as phenyl, alkyl or halohydrocarbon [2]. Recently, researchers elucidated that OPFRs may also become a potential environment problem due to their carcinogenicity, high toxicity and environmental persistence [3,4]. Some specific OPFRs, such as tris(2-chloroethyl) phosphate (TCEP), have high solubility in water (7.943 g L<sup>-1</sup>), which present a significant potential risk to human health. Therefore, it is in urgent need to develop a cost-effective treatment method to remove OPFRs.

Various advanced oxidation processes (AOPs), such as ozonation, Fenton oxidation, TiO<sub>2</sub> photocatalysis and ultraviolet/H<sub>2</sub>O<sub>2</sub> (UV/H<sub>2</sub>O<sub>2</sub>) process, were effective for the elimination of organic contaminants in aqueous medium [5,6]. To date, only a few studies have investigated the degradation of OPFRs using UV/H<sub>2</sub>O<sub>2</sub> systems [7–9], and there is no report about other AOPs. Recently, activated persulfate (PS, S<sub>2</sub>O<sub>8</sub><sup>2-</sup>) is considered as an alternative AOP due to its simple operation, highly oxidizability and wide application. Heating, ultraviolet (UV) illumination and ferrous ion all can activate PS to generate sulfate radical (·SO<sub>4</sub><sup>-</sup>, E<sup>0</sup> = 2.65–3.10 V) [10–12]. However, the addition of ferrous ion will increase the risk of secondary pollution, and the heating has a large demand of energy in actual water treatment. Thus, UV-persulfate (UV/PS) may be more feasible than the other two combinations for actual water treatment. Compared to the non-selective oxidant hydroxyl radical (·OH, E<sup>0</sup> = 2.70–2.80 V), ·SO<sub>4</sub><sup>-</sup> reacts with organic compounds through selective electron-transfer reactions [13], which generate less harmful byproducts [14]. Once the ·SO<sub>4</sub><sup>-</sup> is generated, it can induce a chain of reactions involving the formation of other active species (Eqs. (1)–(5)) [15].



The UV/PS technique with these highly active oxidants may be a potential application for OPFRs elimination; however, there is still no research reports degradation of any OPFR using any PS oxidation, nor to mention the investigation of degradation efficiency, mechanism and safety.

In actual AOPs, a full mineralization of targeted organic contaminants will likely be infeasible due to the operational cost and the competitive reactions of other contaminants [16]. Therefore, a moderate degradation may be feasible in actual water treatment. The determination of degrading intermediates and relevant toxicities can be used to support this application prospect. Recently, a series of toxicological evaluation techniques, such as zebrafish test [17], water flea test [18] and cell line test [19], were applied to investigate the toxicity of OPFRs at cellular level. However, these

techniques did not provide information regarding to the impacts on molecular and metabolic functions, such as gene expression, protein synthesis and signal transduction. The action mechanisms of OPFRs may involve a series of interactions with specific functional proteins and metabolic pathways, thus, the safety assessment of OPFRs degrading products will require a global investigation in the perspective of protein network level.

Within the last decade, the development of isobaric tags for relative and absolute quantitation (iTRAQ) labeling quantitative proteomic technology provided us with a novel and powerful technique that can identify, characterize, and quantify proteins expressed in cells, tissues or organisms under given conditions. Several researches already focused on applying quantitative proteomic for the screening of useful genes and proteins for contaminant degradation in specific microbes [20], or for the toxicology and risk assessment of contaminants [21]. However, there is still no study uses proteomic for the safety evaluation of a contaminant control method. The potential findings in regard to the safety of degrading intermediates on protein network level can provide guidance for the regulation of reaction extent from complete mineralization to a moderate degradation, which may reduce the energy and chemical consumption.

In the current study, 254 nm UV/PS was used for the degradation of TCEP. The degradation effectiveness and intermediates were determined using high resolution mass spectrum (HRMS), and the iTRAQ proteomics analysis was used to evaluate the impacts of TCEP and its degrading intermediate mixture on *Escherichia coli*. This study was expected: (1) to investigate the degradation mechanism of TCEP by UV/PS, (2) to explore the potential application of proteomics for the safety evaluation of AOPs, and (3) to prove the feasibility of applying moderate degradation for TCEP elimination.

## 2. Materials and methods

### 2.1. Chemical reagents and strain

All chemical reagents in the current study were of the highest purity available (Text S1).

### 2.2. UV irradiation module and degradation experiments

A UV irradiation module was designed and assembled. This module consisted of several components, including UV lamp, power source, heat dissipation device, irradiation shield and reactor vessel (Fig. S1). The framework of this module was designed by AutoCAD (Autodesk, USA) and was produced using the laser rapid prototyping technique. The UV light source was a removable low-pressure mercury lamp (power 8 W, effective length 24 cm, Philips, Holland) which had a maximum emitting peak at 254 nm. The irradiating intensity was measured using a HAAS-3000 light spectrum irradiation meter (Everfine, China). The average irradiation intensity was adjusted to 5.0 mW cm<sup>-2</sup> on the surface of reaction solution. A customized circular quartz vessel (12 cm diameter) was used as the reactor vessel.

One hundred milliliters of TCEP solution were spiked into the vessel. In the UV/PS experiments, the initial concentration of Na<sub>2</sub>S<sub>2</sub>O<sub>8</sub> was in the range of 0.83–83.00 mg L<sup>-1</sup> (3.5–350.0 μM). The solution was maintained at 25 ± 2 °C, pH = 6.8–7.2, and its uniformity was achieved by shaking the dish at 60 r min<sup>-1</sup>. The reaction was initiated by turning on the mercury lamp. At a pre-defined time, ascorbic acid, at a concentration that was stoichiometrically equivalent to the initial Na<sub>2</sub>S<sub>2</sub>O<sub>8</sub> dose, was added to stop the reaction. Afterwards, 20 mL of the sample were transferred into a brown amber tube and then stored at 4 °C before sample analysis. The UV-only and PS-only control experiments were included in the

experimental design. In the influence factor experiments, the initial solution pH values were adjusted using phosphate buffer solution (PBS), NaOH and H<sub>3</sub>PO<sub>4</sub> solutions; the predetermined amount of NaNO<sub>3</sub> or humic acid was added in the solution.

### 2.3. Ion chromatography and total organic carbon (TOC) analyses

The determination of Cl<sup>-</sup> and PO<sub>4</sub><sup>3-</sup> was performed using an ICS-2500 analyzer (Dionex, USA) with an ED50A detector. A DIONEX IonPac<sup>®</sup> AS15 column was used with 30.0 mM NaOH solution as the mobile phase. Furthermore, the TOC was measured using a Liq-uid TOC trace analyzer (Elementar, Germany).

### 2.4. Qualitative and quantitative analysis of TCEP and its intermediates

The identification of intermediates was performed using a TripleTOF 5600+ HRMS (Applied Biosystems SCIEX, USA). The quantitative analysis of TCEP and degrading intermediates was performed using a TripleQuad 5500 tandem mass spectrometer (MS<sup>2</sup>) (Applied Biosystems SCIEX, USA). The detailed operational procedure and parameters are presented in Text S2.

### 2.5. Proteomics analysis preparation

The samples for proteomics analysis included: (1) 60 mL 3.5 μM TCEP solution, (2) 60 mL corresponding UV/PS treated sample (intermediate mixture). The reaction condition was set as: temperature 25 ± 2 °C, pH 6.8–7.2, [TCEP]<sub>0</sub> = 3.5 μM, [S<sub>2</sub>O<sub>8</sub><sup>2-</sup>]<sub>0</sub> = 175 μM, reaction time = 30 min. In the proteomics analysis, *E. coli* ATCC11303 was used as the model microorganism, which was inoculated at 100 r min<sup>-1</sup> for 12 h. Subsequently, the cells were obtained by centrifugation at 3500g for 10 min and were washed three times. The cells at 0.1 g L<sup>-1</sup> were inoculated into 20 mL medium containing (in mg L<sup>-1</sup>) 30 KH<sub>2</sub>PO<sub>4</sub>, 70 NaCl, 30 NH<sub>4</sub>Cl, 10 MgSO<sub>4</sub>, 30 beef extract, 100 peptone and 1 TCEP or its intermediate mixture in the dark at 25 °C on a rotary shaker at 100 r min<sup>-1</sup> for 24 h. After exposure, the cells were separated and washed using PBS for protein extraction. The further protein extraction procedure is presented in Text S3.

### 2.6. Protein digestion, iTRAQ labeling and analysis

Briefly, proteins from each sample were reduced with 10 mM DTT for 1 h at 37 °C. The cysteines were blocked with 1 μL blocking reagent for 10 min at room temperature. After then, the samples were centrifuged using 10 KD Amicon Ultra-0.5 filters under 5760g for 20 min. Proteins in filter devices were digested by 50 μL trypsin at 4% w/w overnight at 37 °C. Subsequently, the samples were centrifuged, and 1 μg trypsin was added to each filter for 2 h. After centrifugation, liquid in the collection tube was collected.

The tryptic peptides were labeled with iTRAQ reagent multiplex kit according to the manufacturer's instructions. Subsequently, the labeled peptides were dried in a vacuum concentrator. The samples were then resolved with solution containing 2% v/v acetonitrile and 0.1% v/v formic acid, centrifuged at 5760g for 20 min, and detected by a TripleTOF 5600+ HRMS (Applied Biosystems SCIEX, USA) equipped with a Nanospray III source and a NanoLC 400 system. All HRMS data were combined to search the NCBI database. To avoid false positives, the identified proteins were subjected to an in-house BLAST search at NCBI to confirm the matches. The detailed information of further protein identification is presented in Text S4.

## 3. Results and discussion

### 3.1. Degradation kinetics

The degradation efficiencies of the UV-only, PS-only and UV/PS experiments are presented in Fig. 1a. Slight variations of TCEP were observed both in the PS-only and UV-only experiments, suggesting that inactivated PS had negligible effect on TCEP. This result also indicated that 254 nm UV cannot destruct TCEP by direct photolysis. To the contrary, 254 nm UV/PS induced a significant degradation of TCEP. For 3.5 μM (1 mg L<sup>-1</sup>) TCEP, the removal effectiveness reached ~99% after 30-min reaction ([S<sub>2</sub>O<sub>8</sub><sup>2-</sup>]<sub>0</sub> = 175 μM). Based on the fitting calculation, this degradation was confirmed to be a pseudo-first order reaction (Fig. 1b). The apparent rate constant (*k*<sub>obs</sub>) reached 0.1272 min<sup>-1</sup>, and the half-life was 5.45 min (Table S1), which may be ascribed to the degradation through active radical (such as ·SO<sub>4</sub><sup>-</sup>, ·OH).

The variation of TOC is presented in Fig. 1c. For a 3.5 μM TCEP solution, the apparent TOC value was 0.25 ± 0.03 mg L<sup>-1</sup> at time zero. After 60-min reaction, nearly 54% TOC was removed in the 254 nm UV/PS system, indicating that UV/PS induced a moderate degradation of TCEP. Since a TCEP molecule contains three chlorine terminals and one central phosphorus backbone (Fig. S2), the evolution tendencies of Cl<sup>-</sup> and PO<sub>4</sub><sup>3-</sup> can also describe the degrading pattern of TCEP. The concentration of Cl<sup>-</sup> increased from 0 to 0.37 mg L<sup>-1</sup> after 45-min reaction (Fig. 1d). Theoretically, 3.5 μM TCEP contained approximate 0.37 mg L<sup>-1</sup> chlorine, which was equal to the observed Cl<sup>-</sup> concentration, suggesting a complete cleavage of all C–Cl terminals. Furthermore, PO<sub>4</sub><sup>3-</sup> increased from 0 to 0.13 mg L<sup>-1</sup>, implying that the phosphorus backbone of TCEP was also degraded. However, the theoretical content of PO<sub>4</sub><sup>3-</sup> in 3.5 μM TCEP was 0.33 mg L<sup>-1</sup>, indicating an incomplete degradation. These TOC and ion chromatography results both depicted the incomplete transformation of TCEP, which may generate various intermediates.

### 3.2. Influence factors

Degradation efficiencies of TCEP with different influence factors are presented in Figs. 2 and S3. The related kinetics results are showed in Tables S1–S4. The *k*<sub>obs</sub> of TCEP maintained in the range of 0.1237–0.1495 min<sup>-1</sup> when pH value changed from 3.0 to 9.0, but the *k*<sub>obs</sub> at pH 11.0 (0.0161 min<sup>-1</sup>) was approximately 10 times lower than that at pH 9.0 (Fig. 2, Table S2). Since little difference was observed in the molar absorption coefficients of TCEP with different pH values (Fig. S2), this decreasing efficiency may be attributed to the inhibition of PS reaction. In aqueous matrix, ·SO<sub>4</sub><sup>-</sup> reacts with OH<sup>-</sup> to form ·OH (Eq. (2)). It can be found that when pH ≤ 9.0, the OH<sup>-</sup> ([OH<sup>-</sup>] ≤ 10 μM) in water can only transform partial ·SO<sub>4</sub><sup>-</sup> into SO<sub>4</sub><sup>2-</sup>. However, when pH value increases to 11.0, the [OH<sup>-</sup>] increases to 1000 μM, which can even transform all ·SO<sub>4</sub><sup>-</sup> into SO<sub>4</sub><sup>2-</sup>. Since ·OH can induce non-selective oxidation of TCEP and other contaminants (such as degrading intermediates), the promotion of the substitution reaction of Eq. (2) under alkaline condition will weaken the selective electron-transfer reaction between TCEP and ·SO<sub>4</sub><sup>-</sup>, resulting in the reduction of degradation efficiency. This result suggested that alkaline condition should be avoided in the degradation of TCEP using UV/PS.

Increasing addition of PS had little promotion when [S<sub>2</sub>O<sub>8</sub><sup>2-</sup>] increased from 3.5 μM to 35.0 μM; however, the removal efficiency increased significantly when [S<sub>2</sub>O<sub>8</sub><sup>2-</sup>] increased from 35.0 μM to 350.0 μM. In natural water body, there are many impurities, such as natural organic matters and anions, which may have impacts on the UV-based technique. In the current study, humic acid and NO<sub>3</sub><sup>-</sup> were selected as the representative impurities, and

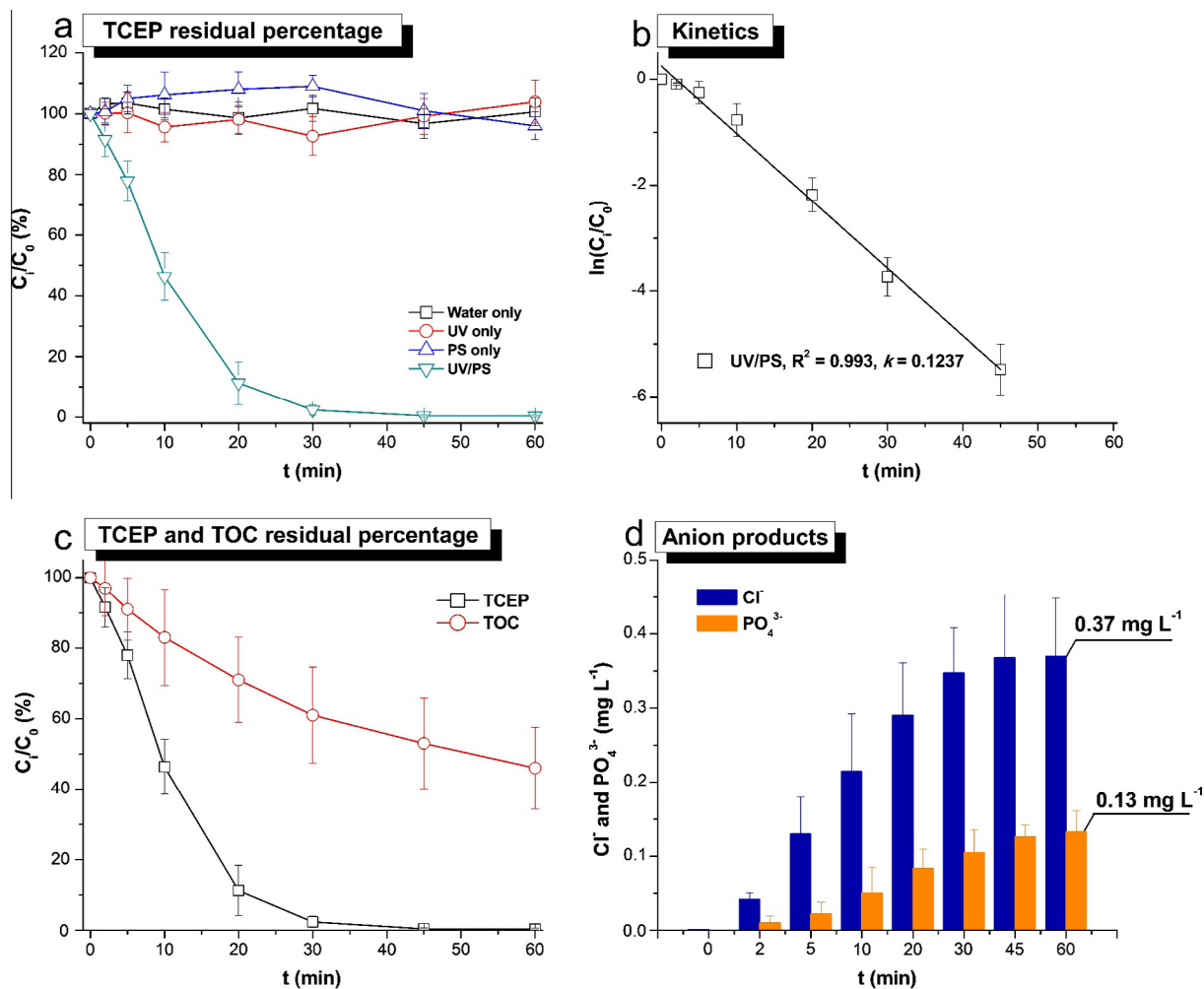


**Fig. 1.** Degradation efficiency of TCEP. Experimental conditions: solution temperature  $25 \pm 2$  °C, pH 6.8–7.2,  $[\text{TCEP}]_0 = 3.5$   $\mu\text{M}$ ,  $[\text{S}_2\text{O}_8^{2-}]_0 = 175$   $\mu\text{M}$  (in PS-only and UV/PS experiments). All the experiments were carried out in triplicate with error bars representing the standard error of the mean.

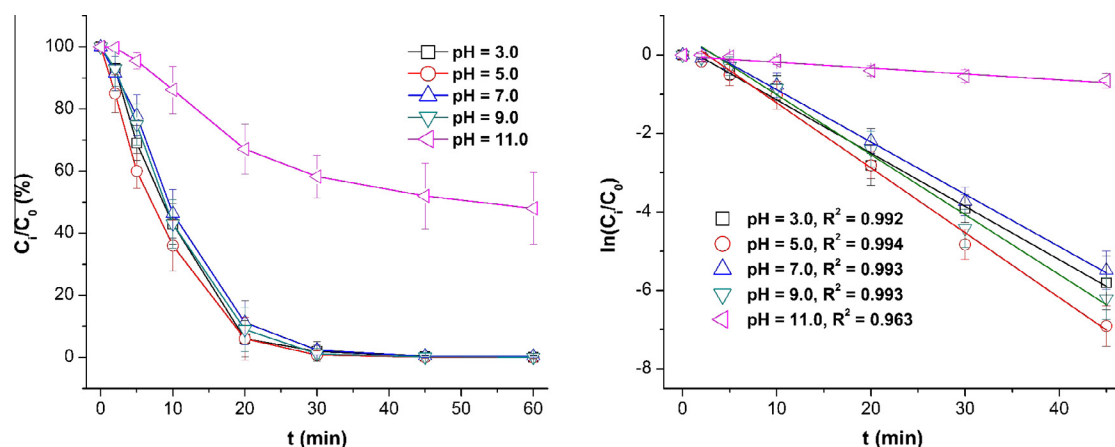


**Fig. 2.** Influence of different pH values in UV/PS experiments. Experimental conditions: solution temperature  $25 \pm 2$  °C,  $[\text{TCEP}]_0 = 3.5$   $\mu\text{M}$ ,  $[\text{S}_2\text{O}_8^{2-}]_0 = 175$   $\mu\text{M}$ . All the experiments were carried out in triplicate with error bars representing the standard error of the mean.

their existences had negative effects on the UV/PS process. As shown in Fig. S3 and Table S3, the  $k_{\text{obs}}$  decreased from  $0.1272$   $\text{min}^{-1}$  (control) to  $0.0458$   $\text{min}^{-1}$  when  $\text{NO}_3^-$  increased to  $100$   $\text{mg L}^{-1}$ . The impact of humic acid was more obvious (Table S4), as the  $k_{\text{obs}}$  decreased to  $0.0045$   $\text{min}^{-1}$  after adding

$100$   $\text{mg L}^{-1}$  humic acid. Humic acid and  $\text{NO}_3^-$  both can absorb UV irradiation, and humic acid can react with  $\cdot\text{SO}_4^-$ , resulting in a decreasing reaction rate. Therefore, the existence of UV screening materials ( $\text{NO}_3^-$ ) and natural organic matters (humic acid) would inhibit the UV/PS degradation of TCEP.

### 3.3. Degradation intermediates and generating mechanism

Based on the molecular structure of TCEP (Fig. S2), two sites, including the C–Cl bond and the central phosphate, may be attacked by the  $\cdot\text{SO}_4^-$ . The screening of potential intermediates from the HRMS data was based on the possible transformations of these sites. Eventually, three steady intermediates were confirmed in the UV/PS experiment. They were identified as  $\text{C}_4\text{H}_9\text{Cl}_2\text{O}_4\text{P}$  (product A,  $m/z$  222.97, 224.97),  $\text{C}_6\text{H}_{13}\text{Cl}_2\text{O}_5\text{P}$  (product B,  $m/z$  266.99, 268.99) and  $\text{C}_2\text{H}_6\text{ClO}_4\text{P}$  (product D,  $m/z$  160.98, 162.97). The observed  $\text{MS}^2$  data and related information of these products are presented in Figs. S4–S6 and Table S6.

Product A (Fig. S4) had a MW of 222.99 Da, which was formed through the cleavage of an ethyl-chlorine arm from the phosphoric center. The generating pathway of product A may involve a three-step reaction (Scheme 1). First, a  $\cdot\text{SO}_4^-$  attacked the phosphoric center, resulting in an addition. Second, a cleavage of one oxygen-ethyl-chlorine arm occurred. Third, through an addition of a  $\text{H}_2\text{O}$  molecule and a chain of electron transport, the  $\cdot\text{SO}_4^-$  ruptured and left behind product A. The further reaction of product A following the same pattern will form product D (Fig. S6), which had a MW of 160.49 Da. After three cycles of this reaction, a TCEP molecule can be degraded to one phosphate radical and other products.

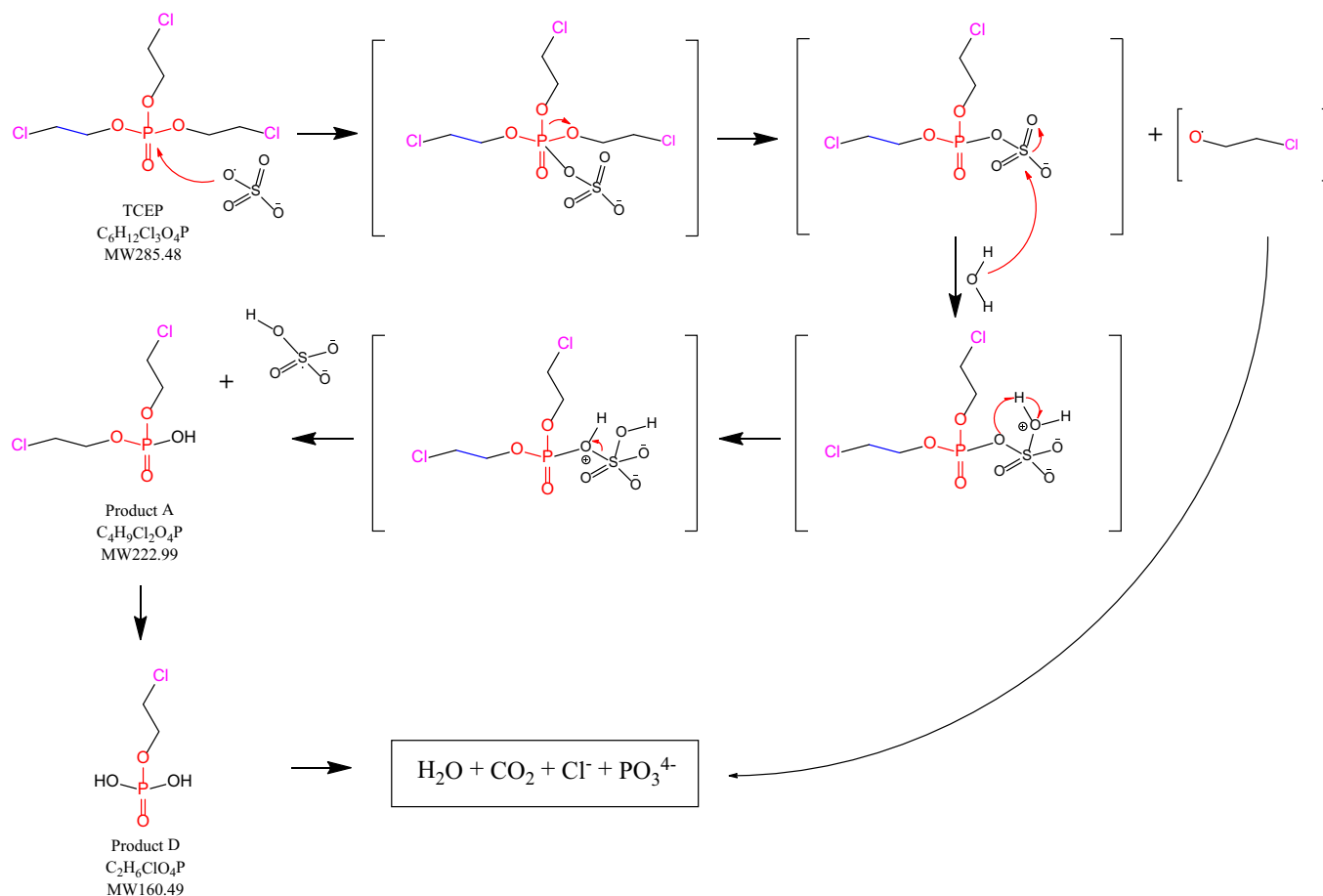
Product B (Fig. S5) had a MW of 267.04 Da, and it had a substitution of one chlorine terminal by a carboxyl. The generating pathway of product B, which may also involve an addition, substitution and rupture process induced by  $\cdot\text{SO}_4^-$ , is presented in Scheme 2. The further degradation of product B may follow the same pattern in Scheme 1. Of note, product C, which was expected to be the further

oxidized intermediate of product B, was not observed in the current reaction.

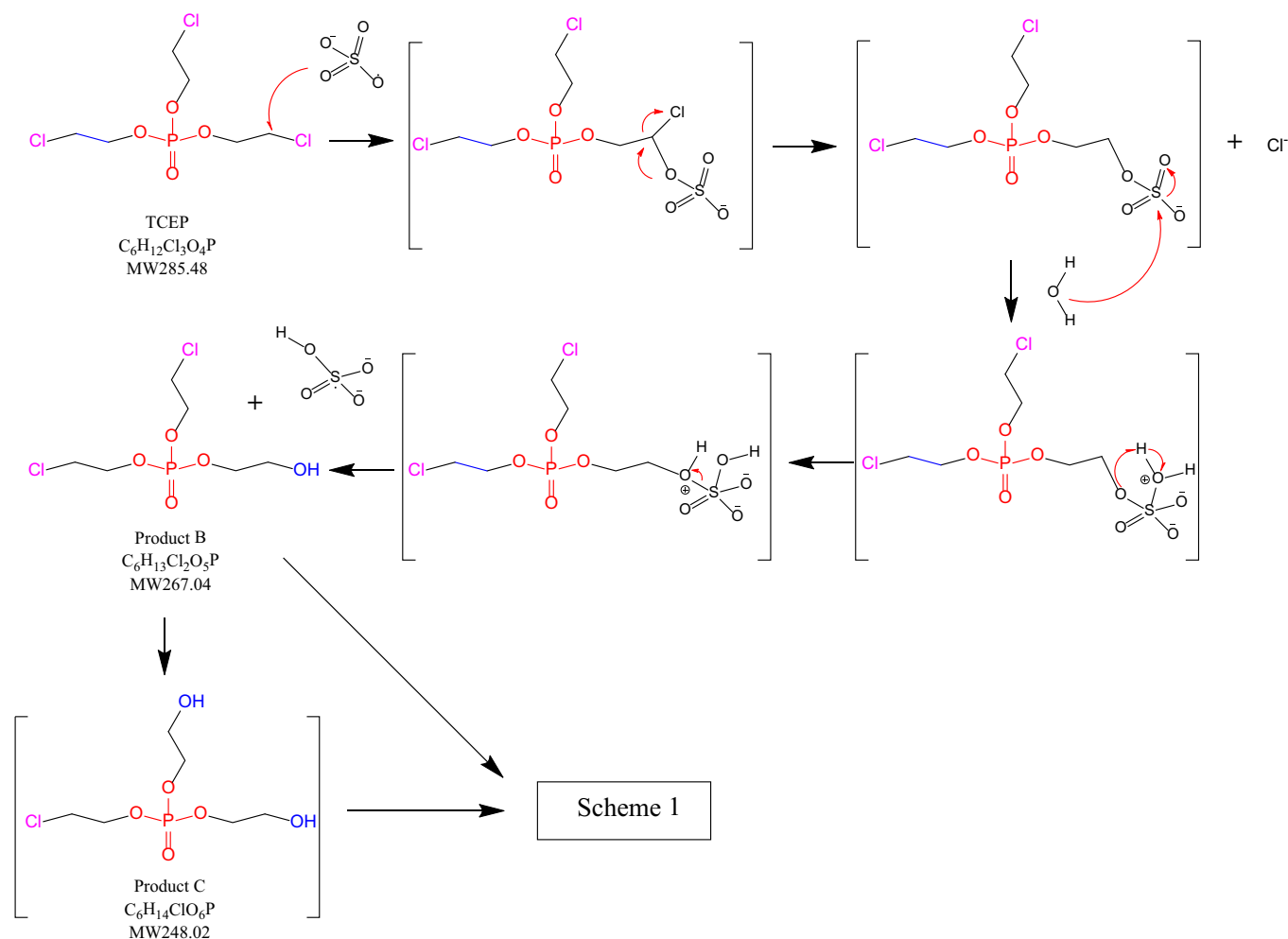
The relative intensity variations and abundance variations of these intermediates are presented in Fig. 3. The intensity of product A increased to approximate  $2.7 \times 10^6$  at 10 min and then showed a decreasing tendency. The intensity of product B showed a similar evolution pattern with a maximum intensity of  $1.2 \times 10^6$  at 10 min. Furthermore, the variation of product D was relative moderate, which increased to  $6.1 \times 10^5$  at 30 min, and then decreased slowly within 60 min. These results confirmed the proposed generative pathway from product A to product D, and it also proved that product A was the dominant intermediate in terms of the relative intensity in 254 nm UV/PS treatment. Of note, all these products gradually decreased and nearly vanished after 60-min reaction, implying that they were transformed into other products. No further degrading product with C–Cl bond was observed in the HRMS data, implying that all the C–Cl bonds were transformed into  $\text{Cl}^-$ . This result was consistent with the generation tendency of  $\text{Cl}^-$  (Fig. 1d).

### 3.4. Biomarkers and functional categories of differently expressed proteins

Among 1135 quantifiable identified proteins (Table S7), 64 (Table S8) and 86 (Table S9) of them were significantly up- and down-regulated expressed in the cells exposed to TCEP intermediate mixture compared to TCEP. Based on the Panther analysis, the molecular functions of the up-regulated expression proteins were binding, catalytic activity, nucleic acid binding transcription factor,



**Scheme 1.** Proposed generative pathways of products A and D after 254 nm UV/PS treatment. Brackets indicate the structures expected, but not detected during experiment.



**Scheme 2.** Proposed generative pathways of products B and C after 254 nm UV/PS treatment. Brackets indicate the structures expected, but not detected during experiment.

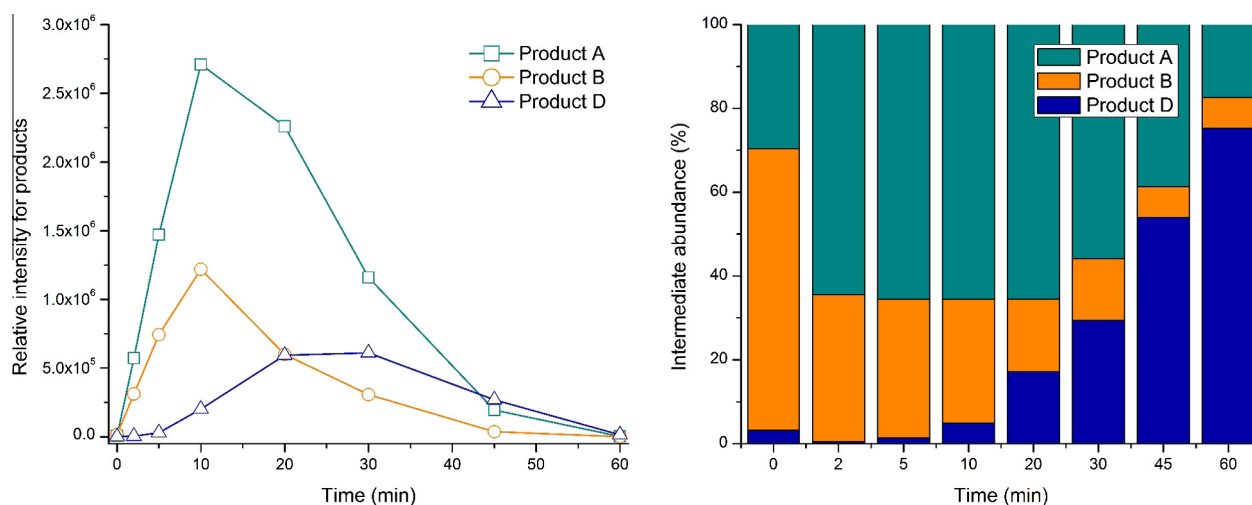


**Fig. 3.** Relative intensity and abundance variations of TCEP organic intermediates in 254 nm UV/PS experiment. Experimental conditions: solution temperature  $25 \pm 2$  °C, pH 6.8–7.2, [TCEP]<sub>0</sub> = 3.5 μM, [S<sub>2</sub>O<sub>3</sub><sup>2-</sup>]<sub>0</sub> = 175 μM. The relative intensity indicates the peak area of extract ion chromatogram from MS/MS data, which has a dimensionless unit.

transporter activity and unknown (Fig. 4a). Besides these functions, some of the down-regulated synthetic proteins were acted as antioxidants, structural molecules and translation regulators. These findings, especially the decreasing expression of proteins associated with antioxidant activity, suggested that the degrading

intermediate mixture imposed less inhibition on the cellular metabolism than intact TCEP. When classified the functions based on the biological processes, the categories of these differentially expressed proteins were biological regulation, cellular process, location, metabolic process and response to stimulus (Fig. 4b).

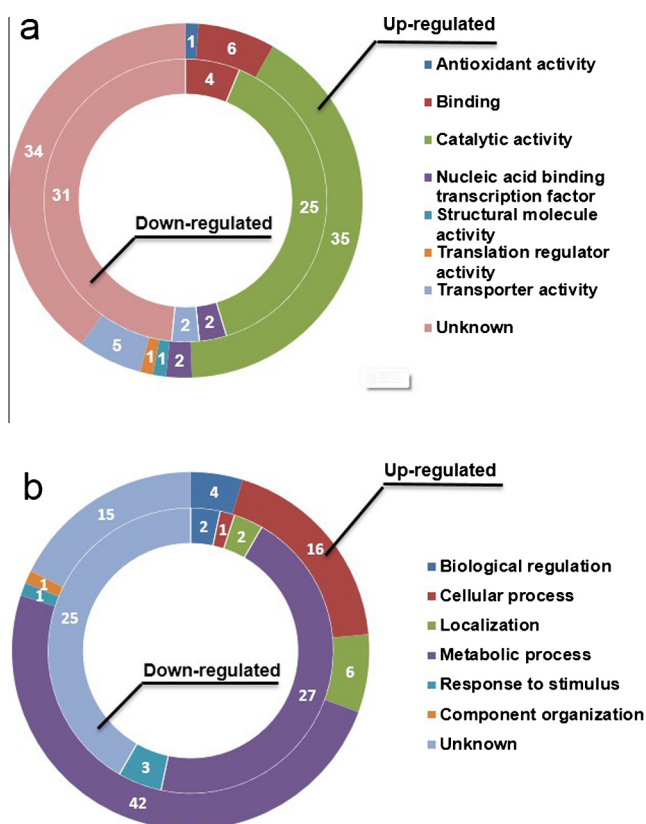


**Fig. 4.** Function categories of differentially expressed proteins in *Escherichia coli* after exposure to UV/PS degrading intermediate mixture compared to TCEP. (a) Molecular functions of up-regulated and down-regulated synthesis proteins, (b) Biological functions of up-regulated and down-regulated synthesis proteins.

Owing to no annotation of some proteins through Panther analysis, String database and KEGG pathway database were used to verify the pathway that each differentiated expressing protein involved (Table S10). The up-regulated expression of the phosphate transporters PhoS, NuoL and NuoK, which related to oxidative phosphorylation, implied the enhancements of energy generation and phosphorus metabolic process (Table S11). However, the decreasing expression of PdxH, AnmK, GmhA, ArnC, Tmk, SthA and YedP associated with phosphorus metabolic process inferred the downward trend of phosphorus metabolism. This finding confirmed that the pathways enriched both up- and down-regulated proteins exhibited diverse activities in different situations. For example, maltose and maltodextrin transport in bacterial chemotaxis pathway was enhanced, whereas dipeptide and ribose import was depressed. For the biosynthesis of amino acids, anthranilate and histidine were increasing expressed, whereas, tryptophan exhibited downward trend. However, the up expressing AroG and down expressing TktB may not trigger the different production of amino acids, because AroG only regulated the transformation of phosphoenolpyruvate and D-erythrose 4-phosphate to 2-dehydro-3-deoxy-D-arabino-heptonate 7-phosphate, and TktB merely catalyzed the reverse transformation among D-ribose 5-phosphate, sedoheptulose 7-phosphate, beta-D-fructose 6-phosphate and D-xylulose 5-phosphate. All of these reactions were just part of the bypasses of the pathway. Therefore, the different expression of these minor proteins may not trigger the metabolic change of some pathways with various bypasses.

To investigate the influence of the degradation intermediate mixture and TCEP on cellular proteomics, the functions of some key proteins were further analyzed. The up-regulated expressed Kch, PstS, ArtJ, SodA, CysJ, Tsr, UspA, NarV, NuoL, NuoK, RibF and

TabA were the biomarkers those related to transport, metabolism and response to stress; while GroL was the biomarker with decreasing concentration.

As a transporter, Kch is an integral membrane protein specific for potassium transport, regulating either by direct binding or physicochemical properties [22]. PstS is a substrate-binding component of the ATP-binding cassette (ABC) transporter complex pstSACB, involving in phosphate and carbon nutrient import [23]. Another ABC transporter ArtJ, which contains SBP\_bac\_3, Lig\_chan-Glu\_bd, NMT1, NMT1.3 and phosphonate-bd motifs, was also responsible for the transport of various substrates across membranes. The up-regulated synthesis of these transporters confirmed that the substrate imports in *E. coli* exposed to the degrading intermediate mixture was significantly improved compared to those in *E. coli* exposed to intact TCEP.

SodA with two iron/manganese superoxide dismutase domains is of great importance for eliminating hydrogen peroxide and superoxide anion, while TabA significantly reduces membrane dispersal [24]. Their up-regulated biosynthesis implied the improved recovery of cells exposure to intermediate mixture compared with TCEP. CysJ is a component of sulfite reductase, containing a flavodoxin motif, a FAD binding domain and an oxidoreductase NAD-binding domain, responsible for the transformation of sulfite to sulfide, which is a key step in the sulfate metabolism [25]. RibF is an essential gene for survival, involving in riboflavin metabolism, which is the key node for lipid, carbohydrate and protein transformation [26].

NADH-quinone oxidoreductase is composed of 14 different protein subunits ([http://www.kegg.jp/kegg-bin/highlight\\_pathway?scale=1.0&map=eco00190&keyword=](http://www.kegg.jp/kegg-bin/highlight_pathway?scale=1.0&map=eco00190&keyword=)), such as NuoL and NuoK, which were identified in the current study. It catalyzes the reversible transfer of electrons from NADH to quinone, a key step of energy conservation in respiratory chain [27]. As for methyl-accepting chemotaxis proteins, *E. coli* has four of them (Tsr, Tar, Trg and Tap) which share a highly conserved signaling and methylation domain. Tsr possess an extracellular domain for monitoring environmental chemo effector levels and an intracellular signaling domain that controls motor responses and undergoes reversible methylation, which enables it to detect chemical changes and transfer signals [28].

Regarding stress response, UspA in *E. coli* plays an important role in oxidative defense and DNA protection inducing by various stresses [29]. Therefore, its up-regulated expression was consistent with the enhanced abundance of SodA, TabA and PstS. As for NarV, it was responsible for the reduction of nitrate to nitrite under anaerobic condition, leading to the generation of a proton motive force and offering *E. coli* the flexibility to survive in the anoxic environments [30].

After TCEP degradation, the up-regulated synthesis of these biomarkers confirmed that the cellular activities associated with potassium, phosphate and carbon nutrient import, sulfur and nitrogen metabolism, energy generation, DNA protection, signal transduction, and anaerobic respiratory were significantly improved. For the down-regulated expression indicator, GroL is a ubiquitous chaperone that is required for correct protein folding, assembly and degradation [31]. Its down-regulated synthesis reflected that the toxicity of TCEP intermediate mixture significantly decreased compared with TCEP because of the reducing wrong expression of proteins.

### 3.5. Proteins related to phospholipid synthesis

Except for active transport through carrier proteins, diffusion across membrane phospholipids is also related to substrate transport. The species and concentrations of phospholipids are associated with diffusion, and are the primary factors that trigger the

changes in membrane permeability [32], which directly determine whether the cells will apoptosis or not. Table S7 showed that the expression of several key enzymes associated with fatty acid formation, including FadA, FadB, FadD, FadH, FadI, FadJ and FadL, did not exhibit significant change. Interaction analysis at String database inferred OmpW, YggL, MipA, Fade, UbiE, MenB, PaaJ, PaaH and Fade were the co-occurrence and neighborhood proteins of these enzymes, showing no obviously different expression. Although the exposure to TCEP and its degradation intermediate mixture significantly changed the synthesis of some membrane-bound proteins and transporters, the above findings indicated that the exposure did not exhibit significant difference on membrane permeability and phospholipid expression in *E. coli*.

### 3.6. Networks of differently expressed proteins

No up-regulated expressing proteins enriched in any network (Fig. S7), whereas, a network among down-regulated proteins was found (Fig. 5), in which GroL and YjeI were two key nodes. The co-occurrence proteins, YjeI, YifE, YajG, YebV, YbhC, YfcZ, YebT, WzzE, Spy, YlaC, YecF, HemY, FdhE and DmsB, in this network were

mainly related to macromolecule and polysaccharide metabolism, heterocycle biosynthesis and sulfur respiration [33,34]. InfA, RpsE, GroL, UspD, DegP, RpoN, PspE, TtcA, MiaB, MnmE, YidC, TolQ, MscL, SspB, ClpB, YbbN, UvrB, IleS and CarA were associated with DNA repair; RNA processing; protein localization, folding and turnover [35]; and response to antibiotic, pollutants, starvation, temperature stimulus and extracellular stimuli [36]. The decreasing expression of these proteins confirmed that the abnormal expression of proteins and DNA under stresses reduced obviously, suggesting the toxicity of the intermediate mixture was significantly lower than that of TCEP.

### 3.7. Cost evaluation

The results of the UV/PS treatment in terms of the removal efficiency and toxicology assessment were observed to be rather good. However, it was also important to evaluate its energy and material cost. The electrical energy per order (EE/O) value was used as an indicator. Detailed procedure of the calculation method was reported in Ref. [37]. The electrical energy cost value (EE/O<sub>e</sub>) was calculated to be 0.0290 kWh m<sup>-3</sup> order<sup>-1</sup> for the 254 nm

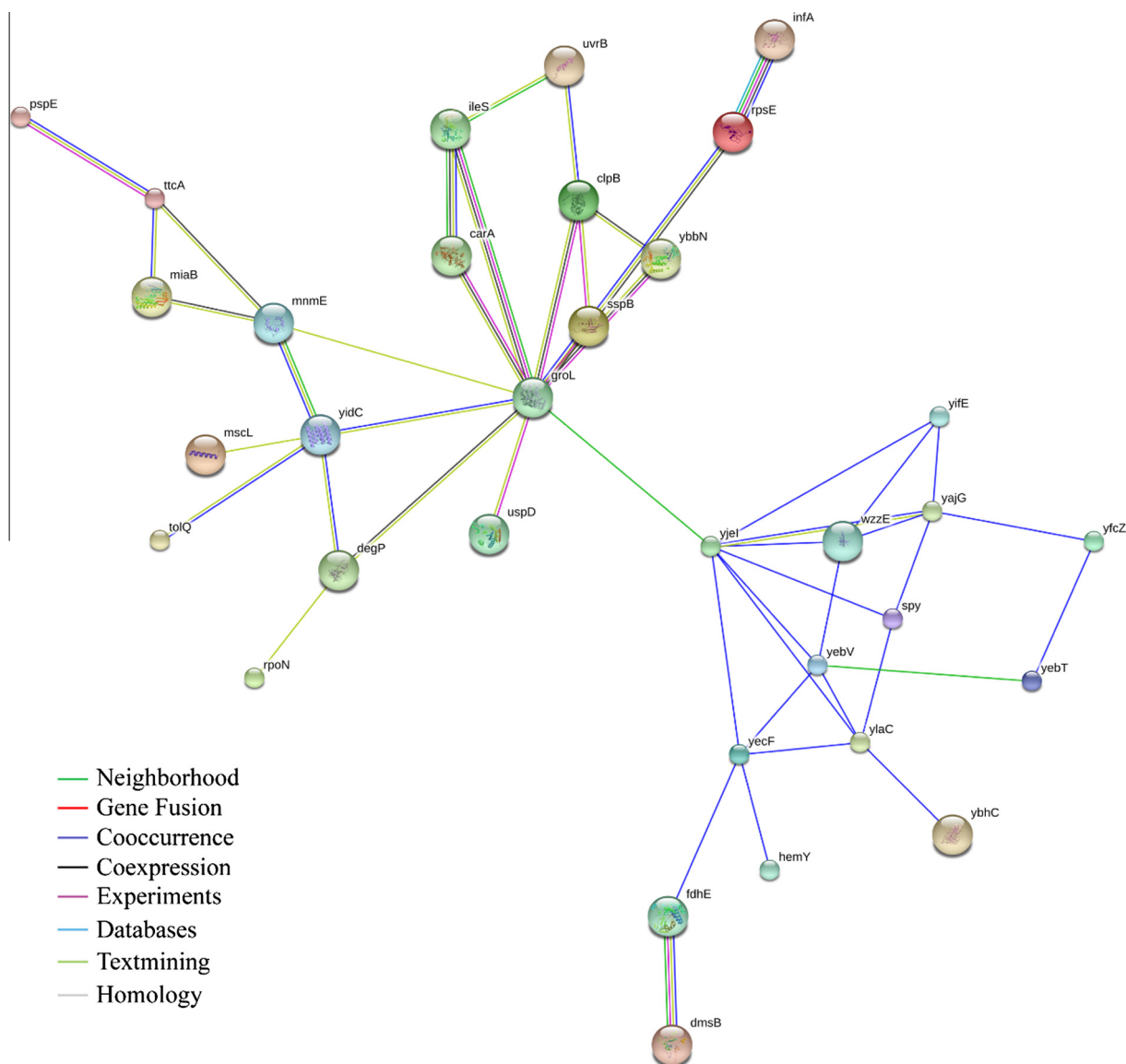


Fig. 5. Biological networks of down-regulated expressed proteins in *E. coli* after exposure to intermediate mixture compared to TCEP.

UV/PS ( $[S_2O_8^{2-}] = 175 \mu\text{M}$ ) treatment (Table S12). For UV/PS treatment with different concentration PS, the chemical oxidant cost value ( $EE/O_c$ , the cost of PS) increased from 0.0004 to  $0.0360 \text{ kWh m}^{-3} \text{ order}^{-1}$  when  $[S_2O_8^{2-}]$  increased from 3.5 to  $350.0 \mu\text{M}$ .

The  $EE/O$  value was calculated by taking into account the  $EE/O_e$  and the  $EE/O_c$  in the UV/PS reactions. Thus, it can be used to represent the overall cost and to guide the optimization of a reaction. Obviously, the total  $EE/O$  decreased from 3.2565 to  $0.0469 \text{ kWh m}^{-3} \text{ order}^{-1}$  as the  $[S_2O_8^{2-}]$  increased from 3.5 to  $175.0 \mu\text{M}$ . When PS concentration increased to  $350 \mu\text{M}$ , the total  $EE/O$  maintained at  $0.0461 \text{ kWh m}^{-3} \text{ order}^{-1}$ , suggesting that there was a relative optimal dosage range (approximate among 175–350  $\mu\text{M}$ ) of PS addition in consideration of the electrical and chemical costs. For the influence factor experiments, the alkaline condition ( $\text{pH} = 11.0$ ) had a significant impact on the total  $EE/O$ , and the existence of humic acid and  $\text{NO}_3^-$  also increased the  $EE/O$  values (Table S10). Since there is no existing report about the cost evaluation of a TCEP degrading reaction, the comparison of  $EE/O$  can only involve the degradation of other contaminants. Compared with the UV/PS treatment of acetaminophen using a low pressure Hg lamp [38], the  $EE/O$  cost for TCEP was higher. Furthermore, the  $EE/O$  values obtained were much higher than the values in a UV-based reaction of ciprofloxacin [39], which had a strong UV absorption. These comparisons implied that TCEP may be a relative robust contaminant against UV-based technique. The application of a moderate degradation, but not complete mineralization, may be a more energy-conservation option for its removal.

#### 4. Conclusion

By adjusting the reaction conditions (such as PS addition dosage and reaction time), the 254 nm UV/PS treatment induced a moderate degradation of TCEP, which had a high transformation efficiency and a relative low mineralization. The qualitative and semi-quantitative analyses demonstrated that the primary intermediates included  $\text{C}_4\text{H}_9\text{Cl}_2\text{O}_4\text{P}$ ,  $\text{C}_6\text{H}_{13}\text{Cl}_2\text{O}_5\text{P}$  and  $\text{C}_2\text{H}_6\text{ClO}_4\text{P}$ . These intermediates were generated by the attack of  $\text{SO}_4^-$  through selective electron-transfer, resulting in an incomplete degradation of TCEP.

After exposure to UV/PS degrading intermediate mixture, the 64 up-regulated proteins were primarily associated with nutrient import/metabolism, energy generation, DNA protection, signal transfer and anaerobic respiratory. The 86 down-regulated proteins were related to DNA repair, protein turnover and stress response, confirming that the toxicity of the degrading intermediate mixture was significantly decreased. The current study provided insights into the molecular mechanisms of TCEP and its degrading products on *E. coli*, clarifying that the UV/PS-based moderate degradation is an effective and safe treatment strategy for TCEP.

#### Acknowledgments

This project was supported by the National Natural Science Foundation of China – China (Grant Nos. 51308224, 21577049), the Science and Technology Planning Project of Guangdong Province, China (Grant Nos. 2014A020216014, 2016A020222005).

#### Appendix A. Supplementary data

Supplementary data associated with this article can be found, in the online version, at <http://dx.doi.org/10.1016/j.cej.2016.09.076>.

#### References

- [1] T. Reemtsma, J.B. Quintana, R. Rodil, M. Garcı, I. Rodrı, Organophosphorus flame retardants and plasticizers in water and air I. Occurrence and fate, *Trac-Trend. Anal. Chem.* 27 (2008) 727–737.
- [2] Å. Bergman, A. Rydén, R.J. Law, J. de Boer, A. Covaci, M. Alaae, L. Birnbaum, M. Petreas, M. Rose, S. Sakai, A novel abbreviation standard for organobromine, organochlorine and organophosphorus flame retardants and some characteristics of the chemicals, *Environ. Int.* 49 (2012) 57–82.
- [3] I. van der Veen, J. de Boer, Phosphorus flame retardants: properties, production, environmental occurrence, toxicity and analysis, *Chemosphere* 88 (2012) 1119–1153.
- [4] G.-L. Wei, D.-Q. Li, M.-N. Zhuo, Y.-S. Liao, Z.-Y. Xie, T.-L. Guo, J.-J. Li, S.-Y. Zhang, Z.-Q. Liang, Organophosphorus flame retardants and plasticizers: sources, occurrence, toxicity and human exposure, *Environ. Pollut.* 196 (2015) 29–46.
- [5] S.C. Pillai, U.L. Stangar, J.A. Byrne, A. Perez-Larios, D.D. Dionysiou, Photocatalysis for disinfection and removal of contaminants of emerging concern, *Chem. Eng. J.* 261 (2015) 1–2.
- [6] A. Matilainen, M. Sillanpää, Removal of natural organic matter from drinking water by advanced oxidation processes, *Chemosphere* 80 (2010) 351–365.
- [7] X.-C. Ruan, R. Ai, X. Jin, Q.-F. Zeng, Z.-Y. Yang, Photodegradation of tri (2-chloroethyl) phosphate in aqueous solution by UV/ $\text{H}_2\text{O}_2$ , *Water Air Soil Pollut.* 224 (2013) 1–10.
- [8] M.J. Watts, K.G. Linden, Photooxidation and subsequent biodegradability of recalcitrant tri-alkyl phosphates TCEP and TBP in water, *Water Res.* 42 (2008) 4949–4954.
- [9] X. Yuan, S. Lacorte, J. Cristale, R.F. Dantas, C. Sans, S. Esplugas, Z. Qiang, Removal of organophosphate esters from municipal secondary effluent by ozone and UV/ $\text{H}_2\text{O}_2$  treatments, *Sep. Purif. Technol.* 156 (2015) 1028–1034.
- [10] Y. Ji, C. Ferronato, A. Salvador, X. Yang, J.-M. Chovelon, Degradation of ciprofloxacin and sulfamethoxazole by ferrous-activated persulfate: implications for remediation of groundwater contaminated by antibiotics, *Sci. Total Environ.* 472 (2014) 800–808.
- [11] C. Tan, N. Gao, D. Yang, W. Rong, S. Zhou, N. Lu, Degradation of antipyrine by heat activated persulfate, *Sep. Purif. Technol.* 109 (2013) 122–128.
- [12] T. An, H. Yang, G. Li, W. Song, W.J. Cooper, X. Nie, Kinetics and mechanism of advanced oxidation processes (AOPs) in degradation of ciprofloxacin in water, *Appl. Catal. B Environ.* 94 (2010) 288–294.
- [13] P. Neta, V. Madhavan, H. Zemel, R.W. Fessenden, Rate constants and mechanism of reaction of sulfate radical anion with aromatic compounds, *J. Am. Chem. Soc.* 99 (1977) 163–164.
- [14] S. Ahn, T.D. Peterson, J. Righter, D.M. Miles, P.G. Tratnyek, Disinfection of ballast water with iron activated persulfate, *Environ. Sci. Technol.* 47 (2013) 11717–11725.
- [15] M. Mahdi-Ahmed, S. Chiron, Ciprofloxacin oxidation by UV-C activated peroxymonosulfate in wastewater, *J. Hazard. Mater.* 265 (2014) 41–46.
- [16] M.C. Dodd, H.-P.E. Kohler, U. Von Gunten, Oxidation of antibacterial compounds by ozone and hydroxyl radical: elimination of biological activity during aqueous ozonation processes, *Environ. Sci. Technol.* 43 (2009) 2498–2504.
- [17] S. Kim, J. Jung, I. Lee, D. Jung, H. Youn, K. Choi, Thyroid disruption by triphenyl phosphate, an organophosphate flame retardant, in zebrafish (*Danio rerio*) embryos/larvae, and in GH3 and FRTL-5 cell lines, *Aquat. Toxicol.* 160 (2015) 188–196.
- [18] S.L. Waaijers, J. Hartmann, A.M. Soeter, R. Helmus, S.A. Kools, P. de Voogt, W. Admiraal, J.R. Parsons, M.H. Kraak, Toxicity of new generation flame retardants to *Daphnia magna*, *Sci. Total Environ.* 463 (2013) 1042–1048.
- [19] N. Ta, C. Li, Y. Fang, H. Liu, B. Lin, H. Jin, L. Tian, H. Zhang, Z. Xi, Toxicity of TDCPP and TCEP on PC12 cell: changes in CAMKII, GAP43, tubulin and NF-H gene and protein levels, *Toxicol. Lett.* 227 (2014) 164–171.
- [20] H. Kjeldal, N.A. Zhou, D. Wissenbach, M. von Bergen, H.L. Gough, J. Nielsen, Genomic, proteomic and metabolite characterization of gemfibrozil-degrading organism *Bacillus* sp. GeD10, *Environ. Sci. Technol.* 50 (2015) 744–755.
- [21] Y. Liu, S. Chen, J. Zhang, B. Gao, Growth, microcystin-production and proteomic responses of *Microcystis aeruginosa* under long-term exposure to amoxicillin, *Water Res.* 93 (2016) 141–152.
- [22] A. Anishkin, S.H. Loukin, J. Teng, C. Kung, Feeling the hidden mechanical forces in lipid bilayer is an original sense, *Proc. Natl. Acad. Sci.* 111 (2014) 7898–7905.
- [23] A. Esteban, M. Díaz, A. Yepes, R.I. Santamaría, Expression of the *pstS* gene of *Streptomyces lividans* is regulated by the carbon source and is partially independent of the PhoP regulator, *BMC Microbiol.* 8 (2008) 1.
- [24] Y. Kim, X. Wang, Q. Ma, X.-S. Zhang, T.K. Wood, Toxin-antitoxin systems in *Escherichia coli* influence biofilm formation through YjgK (TabA) and fimbriae, *J. Bacteriol.* 191 (2009) 1258–1267.
- [25] L. Champier, N. Sibille, B. Bersch, B. Brutscher, M. Blackledge, J. Coves, Reactivity, secondary structure, and molecular topology of the *Escherichia coli* sulfite reductase flavodoxin-like domain, *Biochemistry-us* 41 (2002) 3770–3780.
- [26] X. Wang, Q. Wang, Q. Qi, Identification of riboflavin: revealing different metabolic characteristics between *Escherichia coli* BL21 (DE3) and MG1655, *FEMS Microbiol. Lett.* 362 (2015) fnv071.
- [27] M.A. Spero, F.O. Aylward, C.R. Currie, T.J. Donohue, Phylogenomic analysis and predicted physiological role of the proton-translocating NADH: quinone oxidoreductase (complex I) across bacteria, *mBio* 6 (2015), e00389–00315.

- [28] S.I. Bibikov, A.C. Miller, K.K. Gosink, J.S. Parkinson, Methylation-independent aerotaxis mediated by the *Escherichia coli* Aer protein, *J. Bacteriol.* 186 (2004) 3730–3737.
- [29] T. Su, Q. Wang, L. Yu, C.-A. Yu, Universal stress protein regulates electron transfer and superoxide generation activities of the cytochrome bc<sub>1</sub> complex from *Rhodobacter sphaeroides*, *Biochemistry-us* 54 (2015) 7313–7319.
- [30] P. Ceccaldi, J. Rendon, C. Léger, R. Toci, B. Guigliarelli, A. Magalon, S. Grimaldi, V. Fourmond, Reductive activation of *E. coli* respiratory nitrate reductase, *BBA-Bioenergetics* 1847 (2015) 1055–1063.
- [31] I.N. Naletova, K.M. Popova, M.A. Eldarov, M.L. Kuravsky, E.V. Schmalhausen, I. A. Sevostyanova, V.I. Muronetz, Chaperonin TRiC assists the refolding of sperm-specific glyceraldehyde-3-phosphate dehydrogenase, *Arch. Biochem. Biophys.* 516 (2011) 75–83.
- [32] L. Wang, L. Tang, R. Wang, X. Wang, J. Ye, Y. Long, Biosorption and degradation of decabromodiphenyl ether by *Brevibacillus brevis* and the influence of decabromodiphenyl ether on cellular metabolic responses, *Environ. Sci. Pollut. Res.* 23 (2016) 5166–5178.
- [33] D.P. Kloer, C. Hagel, J. Heider, G.E. Schulz, Crystal structure of ethylbenzene dehydrogenase from *Aromatoleum aromaticum*, *Structure* 14 (2006) 1377–1388.
- [34] C.K. Yu, C.J. Wang, Y. Chew, P.C. Wang, H.S. Yin, M.C. Kao, Functional characterization of *Helicobacter pylori* 26695 sedoheptulose 7-phosphate isomerase encoded by *hp0857* and its association with lipopolysaccharide biosynthesis and adhesion, *Biochem. Biophys. Res. Commun.* 477 (2016) 794–800.
- [35] H. Chi, X. Wang, J. Li, R. Hao, H. Fang, Chaperonin-enhanced *Escherichia coli* cell-free expression of functional CXCR4, *J. Bacteriol.* 231 (2016) 193–200.
- [36] N. Hanna, S. Ouahranibettache, K.L. Drake, L.G. Adams, S. Köhler, A. Occhialini, Global Rsh-dependent transcription profile of *Brucella suis* during stringent response unravels adaptation to nutrient starvation and cross-talk with other stress responses, *BMC Genomics* 14 (2013) 7–10.
- [37] X. He, A. Armah, D.D. Dionysiou, Destruction of cyanobacterial toxin cylindrospermopsin by hydroxyl radicals and sulfate radicals using UV-254nm activation of hydrogen peroxide, persulfate and peroxymonosulfate, *J. Photochem. Photobiol., A* 251 (2013) 160–166.
- [38] C. Tan, N. Gao, S. Zhou, Y. Xiao, Z. Zhuang, Kinetic study of acetaminophen degradation by UV-based advanced oxidation processes, *Chem. Eng. J.* 253 (2014) 229–236.
- [39] H. Ou, J. Ye, S. Ma, C. Wei, N. Gao, J. He, Degradation of ciprofloxacin by UV and UV/H<sub>2</sub>O<sub>2</sub> via multiple-wavelength ultraviolet light-emitting diodes: effectiveness, intermediates and antibacterial activity, *Chem. Eng. J.* 289 (2016) 391–401.